

Research Paper

Simulation of Interstitial Fluid Flow in Ligaments: Comparison among Stokes, Brinkman and Darcy Models

Wei Yao[✉], Zhoufeng Shen and Guanghong Ding

Department of Mechanics and Engineering Science, Fudan University, Shanghai Research Center of Acupuncture, Shanghai, 200433.

✉ Corresponding author: weiyao@fudan.edu.cn.

© Ivyspring International Publisher. This is an open-access article distributed under the terms of the Creative Commons License (<http://creativecommons.org/licenses/by-nc-nd/3.0/>). Reproduction is permitted for personal, noncommercial use, provided that the article is in whole, unmodified, and properly cited.

Received: 2013.07.24; Accepted: 2013.09.27; Published: 2013.11.05

Abstract

In this paper, we use Stokes, Brinkman and Darcy equations to approximate the porous continuum media of ligament tissues respectively, simulate the flow field with FLUENT software, and study the shear stress on the cell surface due to the interstitial fluid flow. Since the Brinkman equation approaches Stokes equation well in high hydraulic permeability (k_p) condition ($k_p \geq 1.0 \times 10^{-8} \text{ m}^2$ in our numerical simulation), and it is an approximation to Darcy model in low k_p condition ($k_p \leq 5.0 \times 10^{-12} \text{ m}^2$ in our numerical simulation), we used the Brinkman model to simulate the interstitial fluid flow in the ligament where k_p is approximately $1.0 \times 10^{-16} \text{ m}^2$. It shows k_p and anisotropic property have a little effect on the flow field, but have a great effect on the shear stress on the membrane of interstitial cells (τ_{cell}). There is a linear relationship between τ_{cell} and $1/\sqrt{k_p}$, when $k_p = 1.0 \times 10^{-16} \text{ m}^2$ and the maximum τ_{cell} ($\tau_{\text{cell,max}}$) is approximately 10 Pa. The anisotropic property will affect τ_{cell} 's distribution on the cell surface. When $k_x/k_y > 1$, low τ_{cell} dominates the cell, while when $k_x/k_y < 1$, high τ_{cell} dominates the cell.

Key words: Interstitial fluid flow, porous media, numerical simulation, shear stress, anisotropy.

Introduction

The interstitium is the space located between the capillary walls and the cells. The basic structure of the interstitium is similar in all tissues: collagen builds a fibril framework that is full of interstitial fluid; interstitial cells are distributed in interstitium. The components of interstitial fluid are very complex, including water, glycosaminoglycan, proteoglycan, proteins and so on. The interstitial fluid volume is as much as approximately 3 times of the blood's volume. Interstitial fluid contacts with the cells more directly than blood does. But the researches on interstitial fluid are fewer than those on blood. Not only the components of interstitial fluid but also its flow plays an important role in the tissue's normal physiological activities [1, 2]. In poorly vascularized tissues such as ligaments and tendons, the flow of interstitial fluid is especially important.

Many factors are known to influence the flow of interstitial fluid. First, interstitial fluid and blood exchange occurs at the capillary walls [3]. Therefore, the flow of interstitial fluid is affected by the conformation of capillaries and the penetrating velocity on the wall of capillaries. Second, the space of the interstitium is not empty but full of collagen fibril network, which affects the flow of interstitial fluid. In different tissues the structure of the collagen fibrils are different. For example, in derma, collagen fibrils are organized into meshes and in ligaments, into regular parallel arrays, as shown in Fig. 1 [4]. Third, interstitial cells also affect the interstitial flow. In brain, neurons and glial cells formed the tight central nervous system (CNS) [5], while in the stained connective tissue, interstitial cells (Mast cells, MCs) are isolated ($\times 400$, Fig.2).

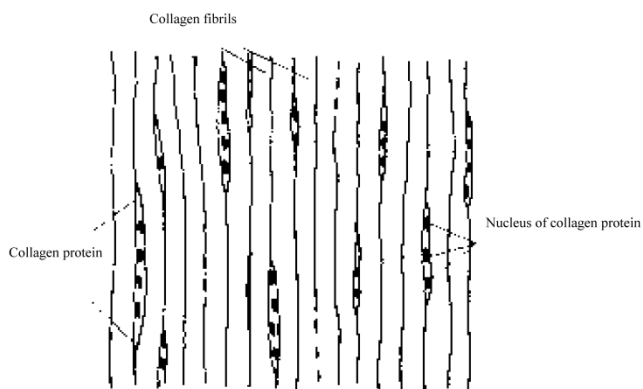


Fig 1. Configuration of parallel collagen fibrils.

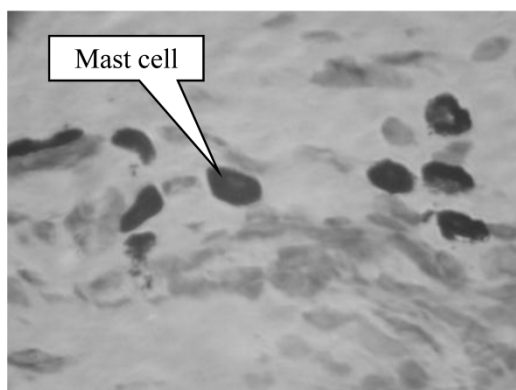


Fig 2. MCs in the skin under electron microscope. One dark circle represents one cell

Most mathematical models of interstitial flow through fibrous matrix to date present the tissue as a continuum space and Stokes, Brinkman and Darcy equations are adopted respectively to study the interstitial fluid flow [6-9]. For example, Lee and Fung [6] used Stokes equation to study a thin boundary-layer region near the fibrils surface. Pedersen et al. [7, 8] and we [9] used Brinkman equation to study the soft tissue. Chen et al. [10] used Darcy equation to study the interstitial fluid flow in ligaments and tendons. In Brinkman and Darcy equations, the properties of the fibrous matrix are represented by a hydraulic permeability k_p that averages the flow resistance offered by the porous media across the entire flow domain. Many factors affect the tissue permeability; therefore, it's hard to determine its accurate value which has to be evaluated in most cases. Yet, through numerical simulation, the estimated values of different cases are widely distinguished, ranging from $1.0 \times 10^{-10} \text{ m}^2$ to $1.7 \times 10^{-17} \text{ m}^2$ [7, 9].

In this paper, based on a simple coupled capillary-interstitium model, we take a computational fluid dynamics (CFD) approach to investigate the following problems: (i) comparison of three equations (Stokes, Brinkman and Darcy) numerical results; (ii) the effect of k_p on the interstitial fluid flow and inter-

stitial cells; (iii) the effect of interstitial cells on the flow field; (iv) the effect of the ratio of longitudinal permeability k_x (parallel to the collagen fibrils) to the transverse permeability k_y (perpendicular to the collagen fibrils) ($ratio = k_x/k_y$) on the interstitial fluid flow and interstitial cells.

Mathematical Model and Methods

Model

The two-dimensional interstitial fluid domain is occupied by a porous media, the top and the bottom of which are the capillaries (Fig.3). The capillaries collocate parallelly in the x direction: the left side of the capillary is near the arteriole, and the right side of the capillary is near the venule. We denote $2H$ as the distance between two neighboring capillaries and L as the length of the capillary. The four short lines at the four corners represent periodic conditions and the lengths of the lines are $0.01 L$.

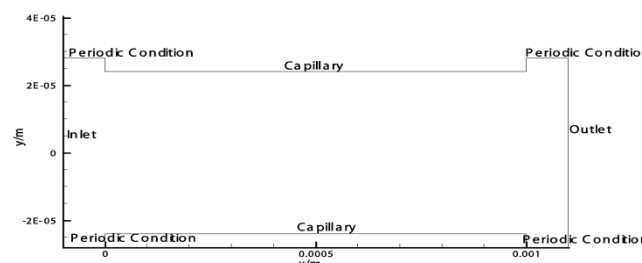


Fig 3. A coupled capillary-interstitium model.

To solve the mathematical model, we need to determine the boundary conditions. Denote $\mathbf{u} = (u_x, u_y)$ the velocity, p the pressure, ρ the density, μ the viscosity. Assuming that before entering and after leaving the domain, the flow is fully-developed and the derivative of horizontal velocities at the inlet and outlet are zero, namely,

$$\frac{\partial u_x}{\partial x} \Big|_{x=-0.01L} = 0, \frac{\partial u_x}{\partial x} \Big|_{x=1.01L} = 0 \quad \dots(1)$$

Unfortunately, these conditions result in the ill-posedness of the problem. To overcome this flaw, we subtract a background flow to fix the horizontal velocity at the inlet ($x=-0.01 L$) to zero. On the other hand, at the top and bottom of the interstitial space, we adopt the well-accepted Starling formula [3]

$$u_y = k_c(p_c - p_i - \pi_c + \pi_i) \quad \dots(2)$$

where k_c is the permeability coefficient of capillary's wall, p_i is the interstitial hydrostatic pressure at the capillary wall, π_c is the osmotic pressure in blood, and π_i is the interstitial osmotic pressure at the capillary

wall. Here, according to the Poiseuille's Law [3], p_c will decrease linearly from artery to vein, assuming other parameters are constants. Finally, we impose the nonslip condition along the capillary walls ($u_x=0$).

In order to study the effect of cells on interstitial flow and the effect of flow on interstitial cells, we place a cell (a circle with diameter of $8\mu\text{m}$) in the center of the domain and impose the nonslip condition on the cell's wall ($u_x=u_y=0$). The sheer stress on the mast cell (τ_{cell}) is

$$\tau_{\text{cell}} = -\mu \left(\frac{\partial u_x}{\partial y} + \frac{\partial u_y}{\partial x} \right)_{\text{cell}} \quad \dots(3)$$

Stokes equation

Assuming the interstitial fluid is incompressible and defining the dimensionless parameters $\mathbf{u}^* = \frac{\mathbf{u}}{U}$, $p^* = \frac{p}{\rho U^2}$, $\mathbf{x}^* = \frac{\mathbf{x}}{D}$, the continuity equation is

$$\nabla \cdot \mathbf{u}^* = 0 \quad \dots(4)$$

where U is the characteristic velocity, defined as $U = k_c[(p_a - p_i) - (\pi_c - \pi_i)]$, p_a is the hydrostatic pressure at the arteriole section of capillary, D is the diameter of capillaries, and ∇ is the gradient operator. Generally, the steady viscous fluid dynamics equation is the Navier-Stokes equation

$$\nabla p^* + \mathbf{u}^* \cdot \nabla \mathbf{u}^* = \frac{1}{\text{Re}} \Delta \mathbf{u}^* \quad \dots(5)$$

where $\text{Re} = \frac{\rho U D}{\mu}$ is the Reynolds number, and Δ is the Laplacian operator. Because Re is small (approximately 10^{-6} in this model), the inertia term ($\mathbf{u}^* \cdot \nabla \mathbf{u}^*$) is negligible compared to the viscous term ($\frac{1}{\text{Re}} \Delta \mathbf{u}^*$). Then the Navier-Stokes equation is simplified as the Stokes equation

$$\nabla p^* = \frac{1}{\text{Re}} \Delta \mathbf{u}^* \quad \dots(6)$$

Brinkman and Darcy equations

Low Reynolds number flows in porous media filled with a matrix of fibrous material have frequently been approximated using a Brinkman equation, and the properties of the material are represented by a hydraulic permeability $\mathbf{k}_p = (k_{px}, k_{py})$ [11]. Pederson et al. [7] evaluated that k_p ranged from approximately $4.0 \times 10^{-11} \text{ m}^2$ to $1.0 \times 10^{-13} \text{ m}^2$ in tissues, while Chen et al. [10] estimated that k_p ranged from $1.0 \times 10^{-16} \text{ m}^2$ to $1.0 \times 10^{-18} \text{ m}^2$ in ligaments. Define $\mathbf{k} = \frac{k_p}{D^2}$, the dimensionless Brinkman equation is

$$\nabla p^* = \frac{1}{\text{Re}} \Delta \mathbf{u}^* - \frac{1}{\text{Re} \cdot \mathbf{k}} \mathbf{u}^* \quad \dots(7)$$

when $|\mathbf{k}|$ is small, the viscous term ($\frac{1}{\text{Re}} \Delta \mathbf{u}^*$) is negligible compared to the Darcy-Forchheimer term ($\frac{1}{\text{Re} \cdot \mathbf{k}} \mathbf{u}^*$) and Brinkman equation reduces to Darcy's law [11],

$$\nabla p^* = -\frac{1}{\text{Re} \cdot \mathbf{k}} \mathbf{u}^* \quad \dots(8)$$

Computational method

The CFD software package FLUENT (version 6.0) is used for the numerical simulation. The grid is generated by the GAMBIT software package. The governing equations are solved by iterating. When the iteration is convergent (error of iterated results $e < 0.001$), the velocity field is obtained.

Physiological parameters

Table 1 shows the physiological parameters used in the numerical simulation. Based on these values, the characteristic velocity $U = 1.33 \times 10^{-6} \text{ m/s}$.

Table 1. Physiological parameter values of the model.

Parameter	Value
Viscosity of interstitial fluid $\mu / (\text{kg m}^{-1} \text{ s}^{-1})$	3.5×10^{-3} [10]
Permeability coefficient of capillary's wall $k_c / (\text{m}^2 \text{ s kg}^{-1})$	5×10^{-10} [13]
Plasma colloid osmotic pressure π_c / mmHg	28 [3]
Interstitial colloid osmotic pressure at the capillary wall π_i / mmHg	8 [12]
Density of interstitial fluid $\rho / (\text{kg m}^{-3})$	1000 [3]
Length of capillary $L / \mu\text{m}$	1000 [3]
Diameter of capillary $D / \mu\text{m}$	8 [3]
Distance between adjacent capillaries $(2H) / \mu\text{m}$	48 [3]
Interstitial hydrostatic pressure at the capillary wall p_i / mmHg	-5 [12]
Hydrostatic pressure at the arteriole section of capillary p_a / mmHg	30 [3]
Hydrostatic pressure at the venule section of capillary p_v / mmHg	10 [3]

Results

Interstitial flow filed in isotropic media

The computational results of Stokes equation and Brinkman equation are nearly the same when k_p is large (Fig.4, $k_p = 1 \times 10^{-8} \text{ m}^2$, display scale is $x:y=1:5$), while the results of Darcy equation and Brinkman equation are similar when k_p is small (Fig.5, $k_p = 5 \times 10^{-12} \text{ m}^2$, display scale is $x:y=1:5$). The numerical results of Stokes, Brinkman and Darcy equations all show that the interstitial fluids flow from the capillary to the interstitium at the arteriole (left) side and are absorbed by the capillaries at the venule (right) side. Near the x axis (symmetry axis, $y=0$), the flows' directions tend to become parallel to the capillaries, and the maximum velocities are at the x axis ($x \approx 660 \mu\text{m}$). The maximum velocities of Stokes and Brinkman ($k_p = 1 \times 10^{-8} \text{ m}^2$) equations are $2.75 \times 10^{-5} \text{ m/s}$, while the maximum velocities of Darcy and Brinkman ($k_p = 5 \times 10^{-12} \text{ m}^2$) equations are $2.01 \times 10^{-5} \text{ m/s}$. The velocity profile in the cross-section causes the difference

between the maximum velocities: the velocity profile of Stokes equation is the parabola shape, which is accordance with Fu et al.'s μ PIV measurement [14] ('+' and 'o' in Fig.6 and Fig.7), while the velocity profile of Darcy equation is nearly equality ('*' and dash-dot line in Fig.6 and Fig.7). The results also show there are boundary layers in Brinkman equation, and the thickness of the boundary layers is positive correlation to k_p ('*' and dash-dot line in Fig.6 and Fig.7).

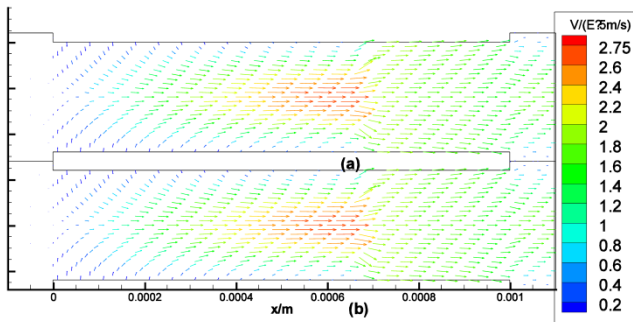


Fig 4. Interstitial flow field in isotropic media (a) Brinkman equation ($k_p=1 \times 10^{-8} m^2$), (b) Stokes equation.

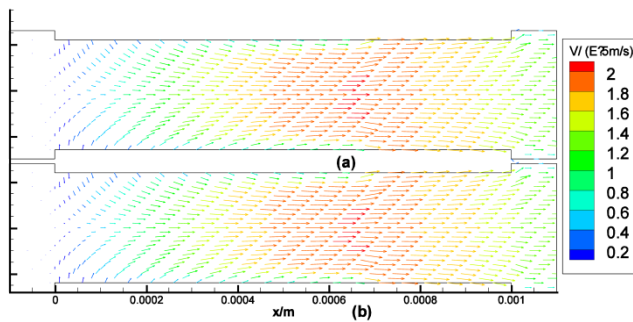


Fig 5. Interstitial flow field in isotropic media (a) Brinkman equation ($k_p=5 \times 10^{-12} m^2$), (b) Darcy equation

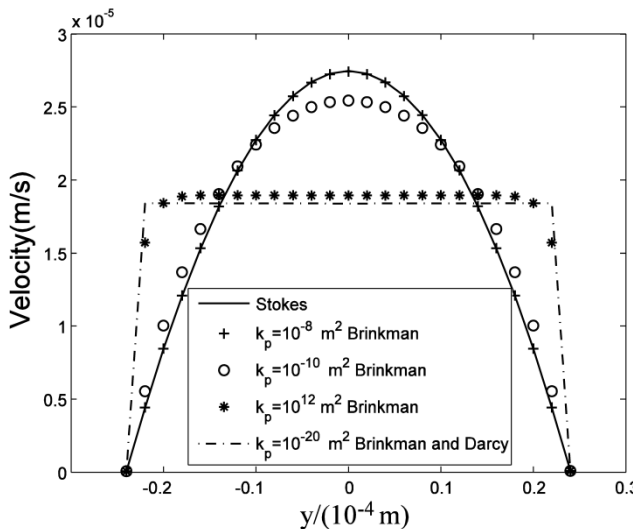


Fig 6. velocity profile in the maximum velocity cross-section ($x=0.66mm$).

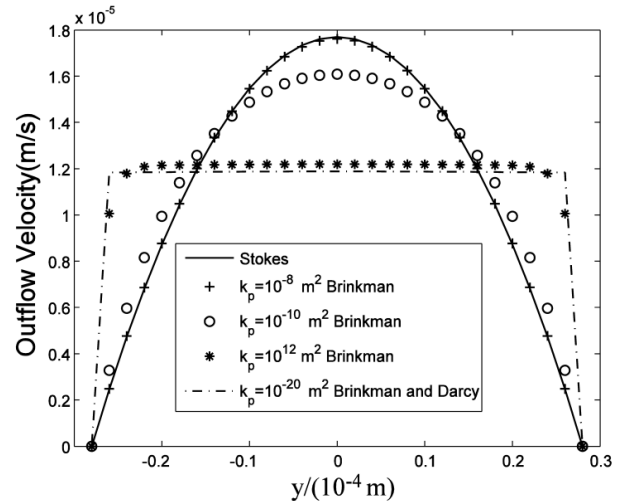


Fig 7. velocity profile at the outlet ($x=1mm$).

The effect of interstitial cells on the flow field

Fig.8 is the flow field near the cell (Brinkman equation, $k_p=1 \times 10^{-12} m^2$). The interstitial cell has little effect on the flow field except for the flow field near the cell surface where a boundary layer exists. Interstitial fluid velocity will provide mechanical stimuli to the interstitial cell, and the shear stress on the surface of cell (τ_{cell}) is direct proportional to $1/\sqrt{k_p}$ because of Brinkman boundary layer (Fig.9). Fig.10 shows the cell's influence is approximately 10 μm range, where '+' and '*' represent the velocities in the cross-sections of 2 μm before and after the cell respectively. There are obviously a large variation at $|y| < 10 \mu m$ range. 'o' represents the velocity in the cross-section of 10 μm before the cell. There is a slightly change at $|y| < 10 \mu m$ range. The solid line represents the velocity in the cross-section of 20 μm before the cell, and it is similar to the velocity without the interstitial cell (dash-dot line in Fig.6).

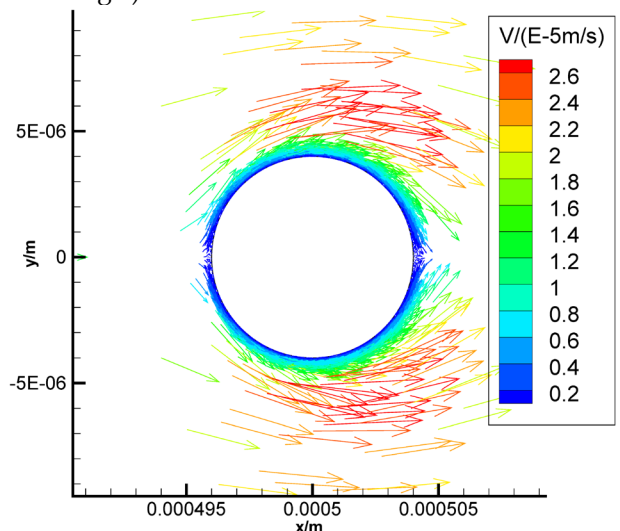


Fig 8. The flow field near the cell (Brinkman equation, $k_p=1 \times 10^{-12} m^2$).

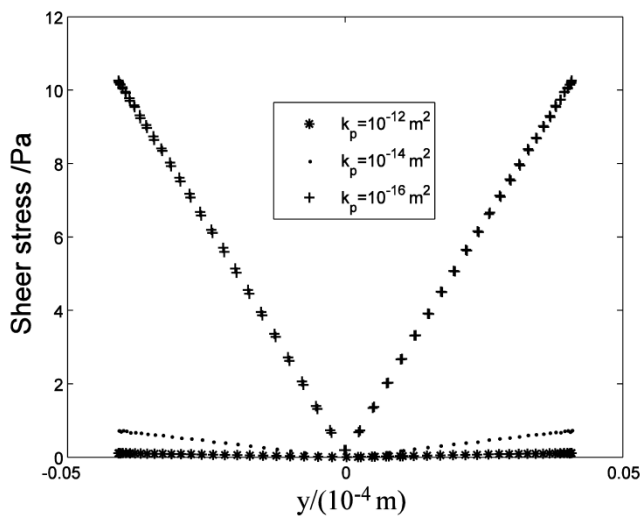


Fig 9. τ_{cell} distribution at the cell surface.

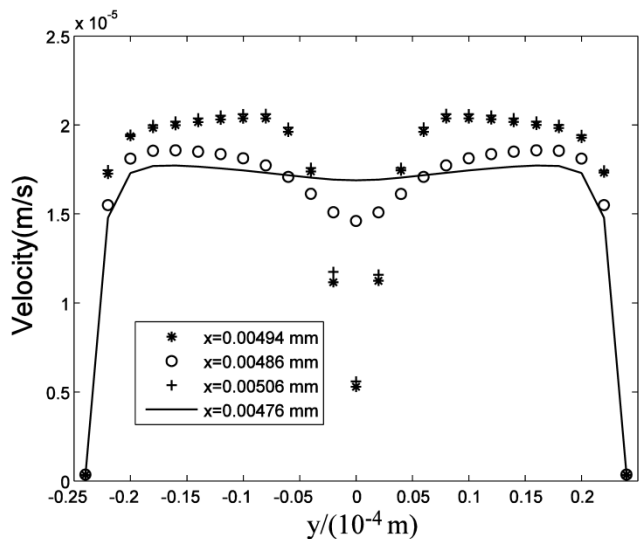


Fig 10. Velocities in the cross-sections.

Interstitial flow filed in anisotropic media

While many researches assumed the tissue is isotropic, Chen et al. [10] showed the parallel arrangement of collagen fibrils in ligaments will certainly lead to anisotropic permeability property in the tissue. Our simulation results showed that the flow fields are similar when k_x is equal to or less than k_y , that is when $k_x/k_y \leq 1$, while the flow fields are different when $k_x > k_y$. Fig.11 is the velocity in the maximum velocity cross-section, which shows the velocity profile is more concave-down with the ratio increase. Fig.12 plots the velocity at the outlet, which shows the velocity profile is more convex with the ratio increase. Though anisotropic property will affect the flow field, Fig.11 and Fig.12 show the influence is less when $k_x/k_y < 10$, and the influence is not great even when

$k_x/k_y=100$. Based on Chen et al.'s results, the maximum evaluation value of *ratio* in ligaments is less than 50 [10]. Therefore, the isotropic analysis in some research is acceptable.

The anisotropic property will affect the flow field near the cell surface and τ_{cell} obviously. Fig.13 shows the low τ_{cell} range increases with *ratio* increasing, and the maximum τ_{cell} is at $y=\pm 4\mu m$ (the top and bottom sides of the cell) when $k_x/k_y > 1$. When $k_x/k_y=100$, τ_{cell} at over 85% range of the cell surface ($y < \pm 3.3 \mu m$) is under 1 Pa, and τ_{cell} increases to 10 Pa quickly near $y=\pm 4\mu m$ position ('.' in Fig.13). When $k_x/k_y < 1$, the positions of maximum τ_{cell} shift to the left and right sides of the cell and the high τ_{cell} range increases ('*' and 'o' in Fig.13, $y=0\mu m$ represent the left and right sides of the cell).

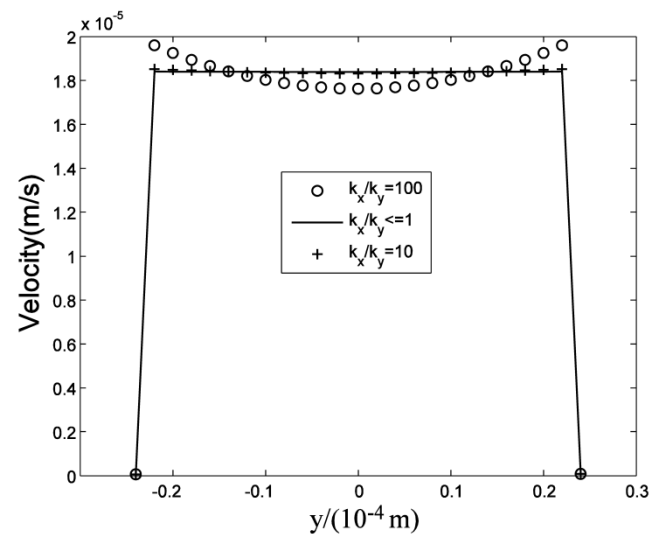


Fig 11. Velocities in the maximum velocity cross-section.

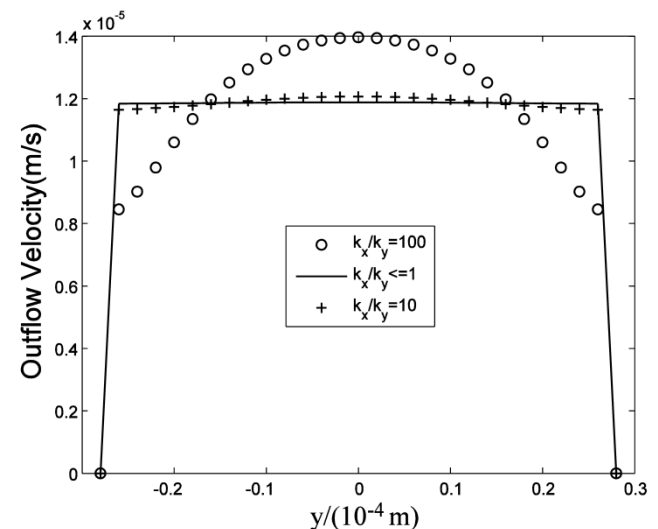


Fig 12. Velocity distribution at the outlet.

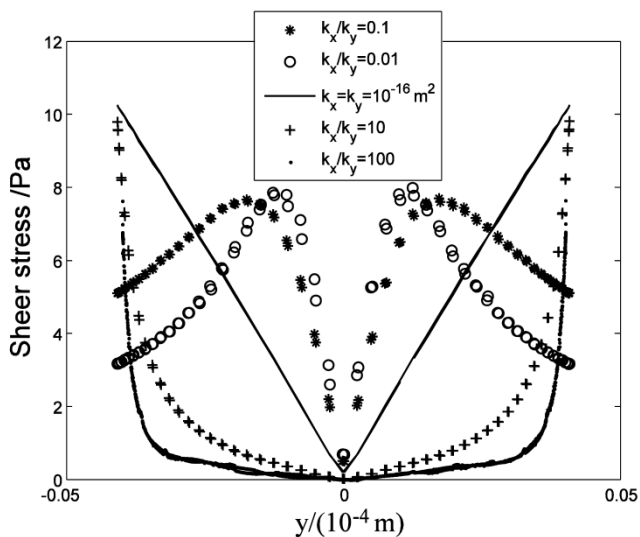


Fig 13. τ_{cell} distribution at the cell surface.

Discussion and Conclusions

In this study, we explore the nature of interstitial fluid flow in ligaments and compare the results derived from Stokes, Brinkman and Darcy models. Through the simulations, we can make the following conclusions.

Parallel array capillaries can induce parallel interstitial fluid flow no matter which model is selected

The interstitial fluid flow is nearly parallel to the capillaries. The difference between these models is the velocity distribution in the cross-section: parabola shape in Stokes model and uniform in Darcy model. The numerical simulation is accordance with the analytical solutions [11]: Brinkman equation approaches Stokes equation well in high k_p condition ($k_p \geq 1.0 \times 10^{-8} \text{ m}^2$), while is an approximation to Darcy model in low k_p condition ($k_p \leq 5.0 \times 10^{-12} \text{ m}^2$), except for that there exist a boundary layer of $\sqrt{k_p}$ magnitude. One group of capillaries will generate $1.2 \times 10^{-5} \text{ m/s}$ (0.07 cm/min) velocity at the outlet. If the fluid from the capillaries is not absorbed by lymphatic, it will flow downstream and be accelerated through the next group of capillaries. In the past, it was accepted that the most seepage from the arteriole side of capillary is absorbed at the venule side of capillary, and the surplus is absorbed by lymphatic vessels right away. Since lymphatic vessels are not always near capillary and the seepage from arteries is always more than the fluid absorbed by capillaries, the unabsorbed fluid will travel some distance and even a long distance before being reabsorbed by capillary or lymphatic. Interstitial fluid flow will affect cells bioactivities. To poorly vascularized tissues such as ligaments and

tendons, the flow of interstitial fluid is more important to metabolism.

Interstitial cells will affect the flow field near the cell surface and interstitial fluid flow can induce shear stress on cell surface

Though the interstitial cell has little effect on the flow field $20 \mu\text{m}$ away from the cell surface, it does affect the flow field near the cell surface. Therefore, for the interstitial cells that isolated from each other (Fig.2), it is reasonable to neglect other cell's effect when study the shear stress on one cell. Interstitial fluid velocity will induce τ_{cell} on the surface of cell in Brinkman equation and τ_{cell} is direct proportional to $1/\sqrt{k_p}$, which is accordance with the theoretical analysis [11].

The anisotropic property has a little effect on the interstitial fluid flow, but will affect τ_{cell} 's distribution on the cell surface

The anisotropic property has little effect on the interstitial fluid flow when $k_x/k_y < 1$, while has some effect on the interstitial fluid flow when $k_x/k_y > 1$. The increase of k_x/k_y will induce the velocity profile concave in the cross-section. We don't know the physiological effect of this concave. Weimbum et al. had found the similar drop in the middle of the cross-section when discussing the flow through an orifice in a fibrous medium [15]. The anisotropic property has obvious effect on τ_{cell} . When $k_x/k_y > 1$, low τ_{cell} dominates the cell and the maximum τ_{cell} is at the top and bottom sides of the cell. When $k_x/k_y < 1$, high τ_{cell} dominates the cell and the positions of maximum τ_{cell} shift to the left and right sides of the cell. This results show that the parallel arrangement of fibril along the capillaries ($k_x/k_y > 1$) can reduce the mechanical stimuli on cells induced by the interstitial fluid flow. In vitro experiments have shown that subtle fluid flow environment plays an important role in cells' living, reproduction and development [16-18]. For example, Swartz et al. found that collagen aligns perpendicular to subtle flow [16], and Hayward et al. figured out that the interstitial fluid velocity and tissue shear stress are key mechanical stimuli for the differentiation of skeletal tissues [18]. But the mechanism of the flow's function is unknown.

This numerical simulation provides an effective way to explore the in vivo interstitial fluid flow in all sorts of tissues, helps to set up the vivid subtle interstitial flow environment of cells, and is benefit to understand the physiological functions of interstitial fluid flow.

Acknowledgement

This work was supported by National natural

science foundation of China (11202053), Shanghai Science Foundation (12ZR1401100), and 973 project (2012CB518502).

Competing Interests

The authors have declared that no competing interest exists.

References

1. Grodzinsky AJ, Levenston ME, Jin M, et al. Cartilage tissue remodeling in response to mechanical forces. *Annu Rev Biomed Eng.* 2000; 2: 691.
2. Swartz MA, Fleury ME. Interstitial Flow and Its Effects in Soft Tissues. *Annu Rev Biomed Eng.* 2007; 9: 229-256.
3. Keener J, Sneyd J. *Mathematical physiology* (Second edition). New York, USA: Springer-Verlag; 2009.
4. Jozsa L, Kannus P, Balini JB, et al. Three-dimensional ultrastructure of human tendons. *Acta Anat.* 1991; 142: 306-312.
5. Abbott NJ. Evidence for bulk flow of brain interstitial fluid: significance for physiology and pathology. *Neurochem Int.* 2004; 45: 545-552.
6. Lee JS, Fung YC. Stokes flow around a circular cylindrical post confined between two parallel plates. *J Fluid Mech.* 1969; 37: 657-670.
7. Pedersen JA, Boschetti F, Swartz MA. Effects of extracellular fiber architecture on cell membrane shear stress in a 3D fibrous matrix. *J Biomech.* 2007; 40: 1484-1492.
8. Pedersen JA, Lichter S, Swartz MA. Cells in 3D matrices under interstitial flow: Effects of extracellular matrix alignment on cell shear stress and drag forces. *J Biomech.* 2010; 43: 900-905.
9. Yao W, Ding GH. Interstitial fluid flow: Simulation of mechanical environment of cells in the interosseous membrane. *Acta Mech Sinica-PRC.* 2011; 27: 602-610.
10. Chen CT, Malkus DS, Vanderby R. A fiber matrix model for interstitial fluid flow and permeability in ligaments and tendons. *Biorheology.* 1998; 35: 103-118.
11. Tsay RY, Weinbaum S. Viscous flow in a channel with periodic cross-bridging fibers: Exact solution and Brinkman approximation. *J Fluid Mech.* 1991; 226:125.
12. Guyton C, Hall JE. *Textbook of Medical Physiology* (Eleventh edition) . Philadelphia, USA: Elsevier Inc; 2006.
13. Hu X, Adamson RH, Liu B, et al. Starling forces that oppose filtration after tissue oncotic pressure is increased. *Am J Physiol-Heart C.* 2000; 279: 1724-1736.
14. Fu Y, Kunz R, Wu JH, et al. Study of Local Hydrodynamic Environment in Cell-Substrate Adhesion Using Side-View μ PIV Technology. *PLOS ONE.* 2012; 7: 1-13.
15. Feng J, Weinbaum S. Flow through an orifice in a fibrous medium with application to fenestral pores in biological tissue. *Chem Eng Sci.* 2001; 56: 5255-5268.
16. Ng CP, Hins B, Swartz MA. Interstitial fluid flow induces myofibroblast differentiation and collagen alignment in vitro. *J Cell Sci.* 2005; 118: 4731.
17. Ng CP, Swartz MA. Mechanisms of interstitial flow-induced remodeling of fibroblast-collagen cultures. *Ann Biomed Eng.* 2006; 34: 446.
18. Hayward LN, Morgan EF. Assessment of a mechano-regulation theory of skeletal tissue differentiation in an in vivo model of mechanically induced cartilage formation. *Biomech Model Mechan.* 2009; 8:447-455.